

Anisotropy effects on heavy quark dynamics in Gribov modified gluon plasma

Sumit,^{1,*} Jai Parkash,^{2,†} Santosh K. Das,^{3,‡} and Najmul Haque^{4,§}

¹*School of Physics, Beijing Institute of Technology, Beijing 102488, China*

²*School of Physics and Astronomy, Shanghai Key Laboratory for Particle Physics and Cosmology, and Key Laboratory for Particle Astrophysics and Cosmology (MOE), Shanghai Jiao Tong University, Shanghai 200240, China*

³*School of Physical Sciences, Indian Institute of Technology Goa, Ponda-403401, Goa, India*

⁴*School of Physical Sciences, National Institute of Science Education and Research, An OCC of Homi Bhabha National Institute, Jatni-752050, India*

In the early stages of relativistic heavy-ion collisions, the momentum distribution of the quark-gluon plasma is anisotropic, leading to instabilities in the system due to chromomagnetic plasma modes. In this work, we consider the anisotropic momentum distribution of the medium constituents to investigate its effects on heavy quark dynamics using the nonperturbative Gribov resummation approach within the framework of the Fokker-Planck equation. Specifically, we study the influence of nonperturbative effects and weak anisotropies on the heavy quark transport coefficients, taking into account the angular dependence between the anisotropy vector and the direction of heavy quark motion. Furthermore, the calculated drag and diffusion coefficients are employed to estimate the energy loss of heavy quarks and the nuclear modification factor, incorporating both elastic collisions and inelastic processes. Our findings indicate that momentum anisotropy, angular dependence, and nonperturbative effects—captured through the scattering amplitudes—play a significant role in determining the transport properties of heavy quarks.

Keywords: Heavy quarks, Momentum anisotropy, diffusion coefficients, quark-gluon plasma

I. INTRODUCTION

Relativistic heavy-ion collisions (HIC) produce a transient state of matter known as the quark-gluon plasma (QGP), which remains in local thermodynamic equilibrium for most of its lifetime [1]. However, the QGP requires a short but finite time to reach this equilibrium state [2], during which the momentum distribution of the pre-equilibrium plasma is generally anisotropic. The partons that are produced in the early stage of these collisions have the momenta along the beam direction, which implies that the longitudinal momenta are enlarged compared to the transverse momenta. Thus, the momentum distribution takes a prolate shape as it becomes strongly elongated along the beam direction. With time, the distribution evolves, and as discussed in Ref. [3], it becomes squeezed along the beam direction, giving an oblate shape. Thus, the characteristic transverse momentum becomes larger than the longitudinal momentum. The QGP state then approaches local equilibrium, although full equilibration is hindered by viscous effects [4]. Hydrodynamic models, which successfully reproduce many experimental observables in HICs, suggest that QGP thermalization occurs rapidly—within less than 1 fm/c [2]. Collective excitations in pre-equilibrium QGP are key to understanding the thermalization scenario, which needs to be fully

understood; see Refs. [5–9] for more details. Although the pre-equilibrium anisotropic phase is very short-lived, it might have a strong effect on the transport coefficients, such as viscosities, diffusion coefficients, and conductivities, which consist of the microscopic properties of the medium. The reason is that the weakly coupled anisotropic QGP is unstable due to color plasma modes, i.e., chromomagnetic fields, which grow exponentially in time and dominate the system dynamics (see recent review [10] for more details).

Heavy flavor particles [11, 12] are one of the important probes used to study the transport properties of QGP because they are produced very early in relativistic HIC. Thus, the heavy quarks (HQs) interact with the bulk medium from the very early stages up to the final stages of the evolution, thereby carrying valuable information about these interactions. This interaction information is generally encoded in the experimental observables such as the nuclear modification factor (R_{AA}) and the elliptic flow (v_2). Experimentally, it has been observed that both R_{AA} and v_2 at large p_T of heavy flavor particles are similar to those of light flavor particles, which confirms that heavy flavor particles interact very strongly with the hot QCD matter [13–15]. Due to their significantly larger masses compared to light quarks, heavy-flavor particles are expected to thermalize more slowly in hot QCD matter. Thus, hydrodynamics is not applicable to studying heavy particles, which are very successful in describing bulk matter dynamics. Within the assumption of soft momentum transfer, the relativistic non-linear Boltzmann equation converts to the Fokker-Planck equation using the diffusion approximation, and also within this approximation, a heavy flavor particle can be treated as a Brownian particle [16].

* sumit@ph.iitr.ac.in

† jaiprakashgagrawal2@gmail.com

‡ santosh@iitgoa.ac.in

§ nhaque@niser.ac.in

To describe the time evolution of heavy flavor particles in hot QCD matter, Langevin or Boltzman transport approaches are utilized under the assumption that the colliding partners from the QGP are in thermal equilibrium [16–24]. However, as discussed, this assumption is not always true in hot QCD matter for the models on which they are applied for several reasons, as follows. (a) Bulk particles also need some finite time to achieve complete thermalization after their production. Also, color-glass condensate [25] theory predicts that the transverse pressure is greater than the longitudinal pressure in the early stages of the HIC. (b) As a consequence of hard scattering at production, the transverse momentum spectra of particles fall off like a power law in HIC at large momenta [26, 27]. (c) Even during the central collisions, there is a corona of nucleons that do not sufficiently scatter to reach the thermal equilibrium and thus can modify the transport coefficients as shown in Ref. [28]. Therefore, in order to compare the calculated transport coefficients with experimental data, it is necessary to include these nonequilibrium effects. Thus, it is helpful to estimate the transport coefficients of HQs when the QGP is not in complete thermal equilibrium. Many studies have been done in this regard to extending the equilibrium scenario [29–44] to nonequilibrium effects [45–62] in HQ transport properties and collective modes studies [63–69]. Recently, the heavy quark diffusion coefficients have been studied in the pre-equilibrium Glasma phase [70–72] (See also [61]).

As discussed earlier, there are strong correlations that have been observed experimentally [13–15] among the heavy flavor particles and the medium constituents, which shows that one needs to go beyond perturbative calculations [17–19] to interpret the experimental data. Several models take into account the nonperturbative aspects [73] through the quasi-hadronic bound states with sequential hadronization from coalescence and fragmentation [74, 75]. Dynamical quasi-particle models are also helpful in studying the transport properties, which take into account the nonperturbative contribution through the lattice thermodynamics results [76–79]. Another strategy to include the nonperturbative effects in HQ dynamics can be done via the Gribov-Zwanziger action [80, 81]. This description includes a scale g^2T known as a (chromo)magnetic scale to include the nonperturbative effects since the perturbative expansion of finite temperature Yang-Mills theory breaks down at this scale, known as the Linde problem [82]. This nonperturbative resummation approach fixes the residual gauge discrepancy in the infrared sector of QCD, which remains after the Faddeev-Popov quantization of QCD, famously known as the Gribov problem [83]. At zero temperature, this approach, with the consideration of the dynamical mass term in gluon and ghost propagator, is quite successful in reproducing the lattice results [84, 85]. For more details on this, look at the recent review [86]. Gribov’s quantization approach has been generalized at finite temperature by Zwanziger, and it has been

shown that the Gribov mass parameter γ_G behaves as a magnetic scale in the asymptotically high-temperature limit [87, 88]. Recently many works have been done in literature in order to comprehend the different properties of deconfined state of matter and to include the non-perturbative aspects in the theory through Gribov picture which brings some interesting outcomes of the corresponding observables [89–100]. For the HQ phenomenology which we are interested in here, HQ potential has been calculated using Gribov approach [101, 102], HQ diffusion coefficient using langevin and Fokker-Planck approach has been studied in Ref. [103, 104], extending the HQ transport coefficients from eikonal to non eikonal scenario in gluon radiation [105] and the energy loss of fast moving parton has been studied in Ref. [106].

In this work, we have extended the HQ momentum evolution, using the Gribov-Zwanziger approach, from isotropic [104] to anisotropic QCD medium and studied the outcomes of momentum anisotropy on HQ transport coefficients, energy loss and the R_{AA} of HQs, using the Gribov-Zwanziger action approach, thus including the nonperturbative aspects in the HQ dynamics. In the anisotropic QCD medium, using the tensor basis, the decomposition of HQ drag coefficient and diffusion coefficient leads to two drag and four diffusion coefficients of HQs contrary to the one drag and two diffusion coefficients in the isotropic medium. The interaction of the HQs with the medium constituents encoded in the matrix elements of the collisional and radiative processes. Gribov propagator provides a natural infrared cut-off in the matrix elements calculation, compared to perturbative approaches, which handle the IR divergences present in t -channel exchange diagrams. Momentum anisotropic effects are included through the nonequilibrium part of the distribution of the constituent particles of the hot QCD medium. We have quantified the effects of momentum anisotropy through the temperature and momentum dependence of HQ transport coefficients by combining both the collisional and radiative processes. It has been deduced that the arbitrary orientation of the direction of anisotropy with respect to HQ momentum and the anisotropy strength plays an important role in quantifying the drag and diffusion properties of HQs.

The work is sketched as follows. After this brief introduction in section I, we discuss the formalism of the HQ drag and diffusion coefficients in the isotropic and anisotropic hot QCD matter in section II. We present results for the HQ drag and diffusion coefficients, utilizing the scattering elements calculated using the Gribov propagator and energy loss of HQs, combining both the collisional and radiative contributions along with the experimental observable R_{AA} in section III. Finally, we summarize the work in section IV. We quote the scattering elements for elastic processes in the appendix A, and different projections between the anisotropic vector and the HQ momentum in the center of mass frame (COM) are presented in appendix B for completeness.

A. Notations and Conventions

The momentum before the collision are $P = (E_p, \mathbf{p})$, $Q = (E_q, \mathbf{q})$ and $P' = (E_{p'}, \mathbf{p}')$ and $Q' = (E_{q'}, \mathbf{q}')$ are momenta after the collision. HQ energy is denoted by $E_p = (|\mathbf{p}|^2 + M_{\text{HQ}}^2)^{1/2}$ whereas the light particles are considered to be massless with $E_q = |\mathbf{q}|$. The quantity $a_k = 1, -1$ refers respectively to the Bose-Einstein and the Fermi-Dirac distributions. The subscript k denotes the different species in the medium.

II. FORMALISM: HEAVY QUARK DRAG AND DIFFUSION IN HOT QCD MEDIUM

The motion of the HQs embedded in a thermal medium can be described through the well-known Fokker-Planck equation described as [16]

$$\frac{\partial f_{\text{HQ}}}{\partial t} = \frac{\partial}{\partial p_i} \left[\mathcal{A}_i(\mathbf{p}) f_{\text{HQ}} + \frac{\partial}{\partial p_j} [\mathcal{B}_{ij}(\mathbf{p}) f_{\text{HQ}}] \right]. \quad (1)$$

Here, f_{HQ} represents the momentum distribution of HQs in the thermal medium and $\mathcal{A}_i(\mathbf{p})$, $\mathcal{B}_{ij}(\mathbf{p})$ denotes the drag and diffusion coefficients of the HQ respectively. We can derive the Fokker-Planck equation from the master Boltzmann equation by applying the Landau approximation. This approximation assumes that the scatterings between the partons in the medium can be considered soft, i.e., the rate of collisions which changes the momentum of the HQ from \mathbf{p} to $(\mathbf{p} - \mathbf{k})$ falls off rapidly with the $|\mathbf{k}|$. In the following section, we discuss the collisional processes in isotropic and anisotropic media and later consider the radiative processes in separate subsections for convenience.

A. Collisional Processes: Isotropic QCD medium

Let us consider the two body elastic interaction processes, i.e., $\text{HQ}(P) + l(Q) \rightarrow \text{HQ}(P') + l(Q')$, where l corresponds to the light particles, i.e. light quarks, light anti-quarks, and gluons. The drag and diffusion tensor can be written in the following manner

$$\begin{aligned} \mathcal{A}_i &= \frac{1}{2E_p} \int \frac{d^3\mathbf{q}}{(2\pi)^3 2E_q} \int \frac{d^3\mathbf{q}'}{(2\pi)^3 2E_{q'}} \int \frac{d^3\mathbf{p}'}{(2\pi)^3 2E_{p'}} \frac{1}{\gamma_{\text{HQ}}} \\ &\times \sum |\mathcal{M}_{2 \rightarrow 2}|^2 (2\pi)^4 \delta^4(P + Q - P' - Q') f_k(E_q) \\ &\times [1 + a_k f_k(E_{q'})] [(\mathbf{p} - \mathbf{p}')_i] = \langle (\mathbf{p} - \mathbf{p}')_i \rangle, \end{aligned} \quad (2)$$

and,

$$\mathcal{B}_{ij} = \frac{1}{2} \langle (\mathbf{p} - \mathbf{p}')_i (\mathbf{p} - \mathbf{p}')_j \rangle. \quad (3)$$

Here, γ_{HQ} denotes the HQ statistical factor and f_k denotes the near-equilibrium distribution function. Also, the delta function dictates the energy conservation for

the two-body scattering process. The scattering amplitude $|\mathcal{M}_{2 \rightarrow 2}|^2$ result is presented in the appendix A. The term $(1 + a_k f_k(E_{q'}))$ represents the Fermi suppression and Bose enhancement regarding the final state particles' phase space. From the Eqs. (2) and (3), it can be seen that the drag coefficient corresponds to the thermal average of the momentum transfer $(\mathbf{p} - \mathbf{p}')$ as an artifact of medium interactions. On the other hand, diffusion coefficients are defined as the average square of the momentum transfer. Since in the isotropic medium, drag and diffusion tensor depend on the HQ momentum only, thus, after using tensorial properties, one obtains the drag coefficient \mathcal{A} as

$$\mathcal{A} = \langle 1 \rangle - \frac{\langle \mathbf{p} \cdot \mathbf{p}' \rangle}{p^2}. \quad (4)$$

While transverse \mathcal{B}_0 and longitudinal \mathcal{B}_1 diffusion coefficient becomes

$$\mathcal{B}_0 = \frac{1}{4} \left[\langle p'^2 \rangle - \frac{\langle (\mathbf{p}' \cdot \mathbf{p})^2 \rangle}{p^2} \right], \quad (5a)$$

$$\mathcal{B}_1 = \frac{1}{2} \left[\frac{\langle (\mathbf{p}' \cdot \mathbf{p})^2 \rangle}{p^2} - 2 \langle \mathbf{p}' \cdot \mathbf{p} \rangle + p^2 \langle 1 \rangle \right]. \quad (5b)$$

Note that the transverse and longitudinal components are identified relative to the HQ momentum. For easiness one do the kinematics study in the COM frame and the average of a generic function $\mathcal{F}(\mathbf{p})$ in COM is given by

$$\begin{aligned} \langle \mathcal{F}(\mathbf{p}) \rangle &= \frac{1}{(512\pi^4) E_p \gamma_{\text{HQ}}} \int_0^\infty q dq \left(\frac{s - M_{\text{HQ}}^2}{s} \right) f_k(E_q) \\ &\times \int_0^\pi d\chi \sin \chi \int_0^\pi d\Theta_{\text{cm}} \sin \Theta_{\text{cm}} \sum |\mathcal{M}_{2 \rightarrow 2}|^2 \\ &\times \int_0^{2\pi} d\Phi_{\text{cm}} [1 + a_k f_k(E_{q'})] \mathcal{F}(\mathbf{p}). \end{aligned} \quad (6)$$

Here, the angle χ defines the relative orientation between the HQ and medium particles in the lab frame, whereas Θ_{cm} and Φ_{cm} represent the polar and azimuthal angles, respectively, in the COM frame. The Mandelstam variables s , t , and u are expressed in terms of particle momenta as:

$$\begin{aligned} s &= (P + Q)^2 = (E_p + E_q)^2 - (p^2 + q^2 + 2pq \cos \chi), \\ t &= (P' - P)^2 = 2p_{\text{cm}}^2 (\cos \Theta_{\text{cm}} - 1), \\ u &= (P' - Q)^2 = 2M_{\text{HQ}}^2 - s - t. \end{aligned} \quad (7)$$

Here $p_{\text{cm}} = |\mathbf{p}_{\text{cm}}|$ is the magnitude of the HQ momentum before the collision in the COM frame. In order to determine the drag and diffusion coefficients, one needs to evaluate the quantity $(\mathbf{p} \cdot \mathbf{p}')$. To that end, the Lorentz transformation, which connects the lab and the COM frame is given by $\mathbf{p}' = \gamma_{\text{cm}} (\mathbf{p}'_{\text{cm}} + \mathbf{v}_{\text{cm}} E'_{\text{cm}})$, where $\gamma_{\text{cm}} = (E_p + E_q)/\sqrt{s}$ and the velocity in the COM is given by $\mathbf{v}_{\text{cm}} = (\mathbf{p} + \mathbf{q})/(E_p + E_q)$. Within COM frame, one can decompose \mathbf{p}'_{cm} as

$$\begin{aligned} \mathbf{p}'_{\text{cm}} &= p_{\text{cm}} (\cos \Theta_{\text{cm}} \mathbf{x}_{\text{cm}} + \sin \Theta_{\text{cm}} \sin \Phi_{\text{cm}} \mathbf{y}_{\text{cm}} \\ &\quad + \sin \Theta_{\text{cm}} \cos \Phi_{\text{cm}} \mathbf{z}_{\text{cm}}), \end{aligned}$$

where $p_{\text{cm}} = (s - M_{\text{HQ}}^2)/(2\sqrt{s})$ is the HQ momentum and $E_{\text{cm}} = (p_{\text{cm}}^2 + M_{\text{HQ}}^2)^{1/2}$ is the energy of the HQ in the COM frame. The axes $\mathbf{x}_{\text{cm}}, \mathbf{y}_{\text{cm}},$ and \mathbf{z}_{cm} are defined as follows $\mathbf{x}_{\text{cm}} = \mathbf{p}_{\text{cm}}/p_{\text{cm}}, \mathbf{y}_{\text{cm}} = N^{-1}(\mathbf{v}_{\text{cm}} - (\mathbf{p}_{\text{cm}} \cdot \mathbf{v}_{\text{cm}})\mathbf{p}_{\text{cm}}/p_{\text{cm}}^2), \mathbf{z}_{\text{cm}} = \mathbf{x}_{\text{cm}} \times \mathbf{y}_{\text{cm}}$ where $N^2 = v_{\text{cm}}^2 - (\mathbf{p}_{\text{cm}} \cdot \mathbf{v}_{\text{cm}})/p_{\text{cm}}^2$. Using these definitions, one can find that

$$\mathbf{p} \cdot \mathbf{p}' = E_p E_p' - \hat{E}_{\text{cm}}^2 + \hat{p}_{\text{cm}}^2 \cos \Theta_{\text{cm}}. \quad (8)$$

B. Collisional Processes: Anisotropic QCD medium

The Momentum distribution of quarks and gluons, which are distributed anisotropically in momentum space, plays a crucial role in determining the state of the medium. An ansatz has been introduced in Ref. [63] to incorporate momentum anisotropy by modifying the isotropic distribution function through a rescaling—either elongation or contraction, along a preferred direction \mathbf{n} , which leads to the momentum distribution of the form

$$f_{\xi}(\mathbf{p}) = C_{\xi} f_0 \left(\sqrt{\mathbf{p}^2 + \xi(\mathbf{p} \cdot \mathbf{n})^2} \right), \quad (9)$$

where $f_0(|\mathbf{p}|)$ is an isotropic distribution of medium constituents, C_{ξ} is a normalization constant and the parameter, $\xi \in (-1, \infty)$ determine the shape of the distribution. When $-1 < \xi < 0$, the momentum distribution is elongated in the direction of \mathbf{n} , resulting in a prolate shape. Conversely, for $\xi > 0$, the distribution is squeezed along the unit vector \mathbf{n} , becoming increasingly oblate as ξ increases. The normalization constant $C_{\xi} = \sqrt{1 + \xi}$ is chosen in such a way that the anisotropic number density matches with the isotropic one. We will consider here $\xi \ll 1$, within this limit the anisotropic distribution function becomes $f_k^{(a)} = f_k^0 + \delta f_k$ with [65]

$$\delta f_k = -\frac{\xi}{2E_q T} (\mathbf{q} \cdot \mathbf{n})^2 (f_k^0)^2 \exp(E_q/T). \quad (10)$$

Here T is the temperature of the thermal bath, and the superscripts ‘a’ and ‘0’ refer to anisotropic and isotropic medium, respectively. Because of the unit vector in an anisotropic medium, contrary to the isotropic one, the drag coefficient can now be decomposed into two different orthogonal vectors as

$$\mathcal{A}_i = p_i \mathcal{A}_0^{(a)} + \tilde{n}_i \mathcal{A}_1^{(a)} \quad (11)$$

where $\tilde{n}^i = \left(\delta_{ij} - \frac{p_i p_j}{p^2} \right) n^j$ such that $\mathbf{p} \cdot \tilde{\mathbf{n}} = 0$. Thus, the two different components of the drag coefficient become

$$\mathcal{A}_0^{(a)} = p_i \mathcal{A}_i / p^2 = \langle 1 \rangle - \frac{\langle \mathbf{p} \cdot \mathbf{p}' \rangle}{p^2}, \quad (12a)$$

$$\mathcal{A}_1^{(a)} = \tilde{n}_i \mathcal{A}_i / \tilde{n}^2 = -\frac{1}{\tilde{n}^2} \langle \tilde{\mathbf{n}} \cdot \mathbf{p}' \rangle. \quad (12b)$$

The new component $\mathcal{A}_1^{(a)}$ consists only anisotropic contribution to the HQ drag coefficient. The average of a function $\mathcal{F}(\mathbf{p}')$ in anisotropic medium can be written as

$$\langle \mathcal{F}(\mathbf{p}') \rangle = \langle \mathcal{F}(\mathbf{p}') \rangle_0 + \langle \mathcal{F}(\mathbf{p}') \rangle_a, \quad (13)$$

where the isotropic contribution $\langle \mathcal{F}(\mathbf{p}) \rangle_0$ is defined in Eq. (6) and the anisotropic contribution $\langle \mathcal{F}(\mathbf{p}) \rangle_a$ can be written analogous to Eq. (6), using the anisotropic distribution function definition, as

$$\begin{aligned} \langle \mathcal{F}(\mathbf{p}) \rangle_a &= \frac{1}{1024\pi^5 E_p \gamma_{\text{HQ}}} \int_0^\infty dq q \left(\frac{s - M_{\text{HQ}}^2}{s} \right) \\ &\times \int_0^\pi d\chi \sin \chi \int_0^{2\pi} d\Phi \int_0^\pi d\Theta_{\text{cm}} \sin \Theta_{\text{cm}} \\ &\times \int_0^{2\pi} d\Phi_{\text{cm}} \left\{ \delta f_k(\mathbf{q}) [1 + a_k f_k^0(\mathbf{q}')] \right. \\ &\left. + a_k f_k^0(\mathbf{q}) \delta f_k(\mathbf{q}') \right\} \mathcal{F}(\mathbf{p}) \sum |\mathcal{M}_{2 \rightarrow 2}|^2. \end{aligned} \quad (14)$$

Similar to Eq. (13), the component of drag force can be written similarly as

$$\mathcal{A}_0^{(a)} = \mathcal{A}_0 + \delta \mathcal{A}_0, \quad (15)$$

having \mathcal{A}_0 as isotropic contribution and $\delta \mathcal{A}_0$ refers to the anisotropic correction to the drag coefficient. Now for the HQ diffusion tensor \mathcal{B}_{ij} , the orthogonal basis can be constructed using the momentum and anisotropy vector as [63]

$$\begin{aligned} \mathcal{B}_{ij} &= \left(\delta_{ij} - \frac{p_i p_j}{p^2} \right) \mathcal{B}_0^{(a)} + \frac{p_i p_j}{p^2} \mathcal{B}_1^{(a)} \\ &+ \frac{\tilde{n}_i \tilde{n}_j}{\tilde{n}^2} \mathcal{B}_2^{(a)} + (p^i \tilde{n}^j + p^j \tilde{n}^i) \mathcal{B}_3^{(a)}. \end{aligned} \quad (16)$$

The different diffusion components can be obtained via the proper projection of Eq. (16) as [53]

$$\begin{aligned} \mathcal{B}_0^{(a)} &= \frac{1}{2} \left[\left(\delta_{ij} - \frac{p_i p_j}{p^2} \right) - \frac{\tilde{n}_i \tilde{n}_j}{\tilde{n}^2} \right] \mathcal{B}_{ij} \\ &= \frac{1}{4} \left[\langle p'^2 \rangle - \frac{\langle (\mathbf{p}' \cdot \mathbf{p})^2 \rangle}{p^2} - \frac{\langle (\mathbf{p}' \cdot \tilde{\mathbf{n}})^2 \rangle}{\tilde{n}^2} \right], \end{aligned} \quad (17a)$$

$$\begin{aligned} \mathcal{B}_1^{(a)} &= \frac{p_i p_j}{p^2} \mathcal{B}_{ij} \\ &= \frac{1}{2} \left[\frac{\langle (\mathbf{p}' \cdot \mathbf{p})^2 \rangle}{p^2} - 2 \langle (\mathbf{p}' \cdot \mathbf{p}) \rangle + p^2 \langle 1 \rangle \right], \end{aligned} \quad (17b)$$

$$\begin{aligned} \mathcal{B}_2^{(a)} &= \left[\frac{2\tilde{n}_i \tilde{n}_j}{\tilde{n}^2} - \left(\delta_{ij} - \frac{p_i p_j}{p^2} \right) \right] \mathcal{B}_{ij} \\ &= \frac{1}{2} \left[-\langle p'^2 \rangle + \frac{\langle (\mathbf{p}' \cdot \mathbf{p})^2 \rangle}{p^2} + \frac{2 \langle (\mathbf{p}' \cdot \tilde{\mathbf{n}})^2 \rangle}{\tilde{n}^2} \right], \end{aligned} \quad (17c)$$

$$\begin{aligned} \mathcal{B}_3^{(a)} &= \frac{1}{2p^2 \tilde{n}^2} (p^i \tilde{n}^j + p^j \tilde{n}^i) \mathcal{B}_{ij} \\ &= \frac{1}{2p^2 \tilde{n}^2} [-p^2 \langle (\mathbf{p}' \cdot \tilde{\mathbf{n}}) \rangle + \langle (\mathbf{p}' \cdot \mathbf{p}) (\mathbf{p}' \cdot \tilde{\mathbf{n}}) \rangle]. \end{aligned} \quad (17d)$$

where $\tilde{n}^2 = 1 - ((\mathbf{p} \cdot \hat{\mathbf{n}})^2/p^2) = 1 - \cos^2 \Theta_n$. To determine the quantity in COM frame $\langle \tilde{\mathbf{n}} \cdot \mathbf{p}' \rangle$, one can consider $\mathbf{n} = (\sin \Theta_n, 0, \cos \Theta_n)$, where angle Θ_n is the angle between anisotropy vector and the HQ momentum direction which is chosen as $\mathbf{p} = (0, 0, p)$. Also, light quark momentum can be decomposed as $\mathbf{q} = (q \sin \chi \cos \Phi, q \sin \chi \sin \Phi, q \cos \chi)$. Thus we have

$$\begin{aligned} \mathbf{p} \cdot \mathbf{q} &= pq \cos \chi, & \mathbf{p} \cdot \mathbf{n} &= p \cos \Theta_n \\ \mathbf{q} \cdot \mathbf{n} &= q \sin \chi \cos \Phi \sin \Theta_n + q \cos \chi \cos \Theta_n. \end{aligned} \quad (18)$$

Further, using the definition of \tilde{n}^i , we can define

$$\langle \tilde{\mathbf{n}} \cdot \mathbf{p}' \rangle = \langle \mathbf{n} \cdot \mathbf{p}' \rangle - \langle \mathbf{p} \cdot \mathbf{p}' \rangle \frac{\cos \Theta_n}{p}. \quad (19)$$

After doing some simplification, the Eq. (19) takes the form

$$\begin{aligned} \tilde{\mathbf{n}} \cdot \mathbf{p}' &= \frac{\gamma_{cm}}{1 + \gamma_{cm}^2 v_{cm}^2} \left\{ p_{cm} [\cos \Theta_{cm} (\mathbf{x}_{cm} \cdot \mathbf{n}) + \sin \Theta_{cm} \sin \Phi_{cm} \right. \\ &\quad \times (\mathbf{y}_{cm} \cdot \mathbf{n}) + \sin \Theta_{cm} \cos \Phi_{cm} (\mathbf{z}_{cm} \cdot \mathbf{n})] \\ &\quad \left. + \gamma_{cm} E'_p \frac{p \cos \Theta_n + q \cos \chi \cos \Theta_n + q \sin \chi \cos \Phi \sin \Theta_n}{E_p + E_q} \right\} \\ &\quad - \frac{\gamma_{cm}}{1 + \gamma_{cm}^2 v_{cm}^2} \frac{\cos \Theta_n}{p} \left\{ \hat{p}_{cm} [\cos \Theta_{cm} (\mathbf{x}_{cm} \cdot \mathbf{p}) \right. \\ &\quad \left. + \sin \Theta_{cm} \sin \Phi_{cm} (\mathbf{y}_{cm} \cdot \mathbf{p})] + \gamma_{cm} E'_p \frac{p(p + q \cos \chi)}{E_p + E_q} \right\}, \end{aligned} \quad (20)$$

where the different projections of Eq. (20) are mentioned in appendix B.

C. Radiative Process

In addition to elastic $2 \rightarrow 2$ scattering processes, gluon radiation in the medium is also possible, as illustrated in Fig. 1. Such radiative processes play a significant role in estimating the transport properties of HQs. An example of this is the inelastic scattering process: $\text{HQ}(P) + l(Q) \rightarrow \text{HQ}(P') + l(Q') + g(K')$, where $K' = (E_{k'}, \mathbf{k}'_\perp, k'_z)$ denotes the four-momentum of the soft gluon emitted by the HQ in the final state of the interaction. The general expression for these $2 \rightarrow 3$ inelastic processes can be derived by substituting the two-body phase space factor and scattering amplitude with their respective three-body counterparts. This allows for the computation of the thermally averaged quantity $\langle \mathcal{F}(\mathbf{p}) \rangle$ for inelastic processes as

$$\begin{aligned} \langle \mathcal{F}(\mathbf{p}) \rangle_{\text{rad}} &= \frac{1}{2E_p \gamma_{\text{HQ}}} \int \frac{d^3 \mathbf{q}}{(2\pi)^3 E_q} \int \frac{d^3 \mathbf{q}'}{(2\pi)^3 E_{q'}} \int \frac{d^3 \mathbf{p}'}{(2\pi)^3 E_{p'}} \\ &\quad \times \int \frac{d^3 \mathbf{k}'}{(2\pi)^3 E_{k'}} \sum |\mathcal{M}_{2 \rightarrow 3}|^2 f_k(E_q) (1 \pm f_k(E_{q'})) \\ &\quad \times (1 + f_g(E_{k'})) \Theta(E_p - E_{k'}) \Theta(\tau - \tau_F) \\ &\quad \times \mathcal{F}(\mathbf{p}) (2\pi)^4 \delta^{(4)}(P + Q - P' - Q' - K'). \end{aligned} \quad (21)$$

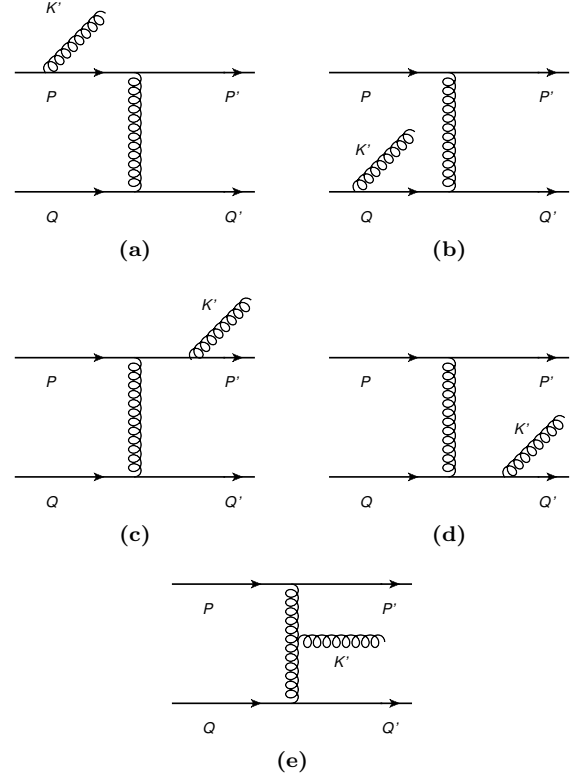


FIG. 1: Feynman diagrams for process $\text{HQ}(P) + l(Q) \rightarrow \text{HQ}(P') + l(Q') + g(K')$, showing the radiative processes of the HQ scattering with light quark and a soft gluon radiation.

Here, the scattering duration, which characterizes the time between successive interactions of the HQs with the medium constituents, is represented by τ , and τ_F represents the gluon formation timescale. The Θ function imposes constraints on the dynamics of emitted gluons within the medium. Specifically, the condition $\Theta(E_p - E_{k'})$ ensures the emitted gluon's energy is less than the initial energy of the HQ. At the same time, $\Theta(\tau - \tau_F)$ puts the constraint that the formation time of gluon should be less than the interaction time of the HQ with the medium constituents and thus accounting for the Landau-Pomeranchuk-Migdal (LPM) suppression effect [41–43]. Also, $f_g(E_{k'}) = 1/[\exp(\beta E_{k'}) - 1]$ is the distribution of the radiated gluon where $\beta = 1/T$. It is assumed that the radiated gluon is in a thermally equilibrated state. The interaction term $|\mathcal{M}_{2 \rightarrow 3}|^2$ for the $2 \rightarrow 3$ radiative process can be expressed through the interaction term for the elastic process times the probability for soft gluon emission [44] as follows,

$$|\mathcal{M}_{2 \rightarrow 3}|^2 = |\mathcal{M}_{2 \rightarrow 2}|^2 \times \frac{48\pi\alpha_s(T)}{k_1'^2} \left(1 + \frac{M_{\text{HQ}}^2}{s} e^{2\zeta} \right)^{-2}, \quad (22)$$

where $\alpha_s(T)$ is the strong running coupling defined up to one-loop as

$$\alpha_s(T) = \frac{6\pi}{11N_c - 2N_f} \frac{1}{\ln(2\pi T/\Lambda_{\text{MS}})} \quad (23)$$

having scale $\Lambda_{\overline{\text{MS}}} = 176 \text{ MeV}$ [107] for $N_f = 3$. Additionally, ζ represents the rapidity of the emitted gluon, and the term $(1 + M_{\text{HQ}}^2 e^{2\zeta}/s)^{-2}$ acts as a suppression factor for the HQ due to the dead-cone effect [29, 44]. Consequently, from Eq. (21), we obtain

$$\langle\langle \mathcal{F}(\mathbf{p}) \rangle\rangle_{\text{rad}} = \langle\langle \mathcal{F}(\mathbf{p}) \rangle\rangle_{\text{coll.}} \times \mathcal{I}(\mathbf{p}), \quad (24)$$

where $\mathcal{I}(\mathbf{p})$ is given by

$$\begin{aligned} \mathcal{I}(\mathbf{p}) = & \int \frac{d^3 k'}{(2\pi)^3 2E_{k'}} \frac{48 \alpha_s(T)}{k_{\perp}'^2} \left(1 + \frac{M_{\text{HQ}}^2}{s} e^{2\eta}\right)^{-2} \\ & \times (1 + \mathfrak{f}_g(E_{k'})) \Theta(E_p - E_{k'}) \Theta(\tau - \tau_F). \end{aligned} \quad (25)$$

The Eq. (25) can be simplified further by noting the relations between the energy and transverse momentum of the emitted gluon with the rapidity variable as follows:

$$E_{k'} = k_{\perp}' \cosh \zeta, \quad k_z' = k_{\perp}' \sinh \zeta, \quad (26)$$

with $d^3 k' = d^2 k_{\perp}' dk_z' = 2\pi k_{\perp}'^2 dk_{\perp}' \cosh \zeta d\zeta$. The interaction time τ is related to the interaction rate $\Gamma = 2.26\alpha_s T$ and the $\Theta(\tau - \tau_F)$ impose the constraint $\tau = \Gamma^{-1} > \tau_F = (\cosh \zeta)/(k_{\perp}')$ which puts a lower cut-off on k_{\perp}' . While the other theta function i.e. $\Theta(E_p - E_{k'})$ constraint the upper limit of $(k_{\perp}')_{\text{max}} = (E_p)/\cosh \zeta$. Thus in the limiting case ($E_{k'} \ll T$), the integral $\mathcal{I}(\mathbf{p})$ becomes

$$\begin{aligned} \mathcal{I}(\mathbf{p}) = & \frac{6}{\pi} \alpha_s T \int_{\Gamma \cosh \zeta}^{E_p/\cosh \zeta} dk_{\perp}' \int_{-\zeta_1}^{\zeta_1} d\zeta \\ & \times \left(1 + \frac{M_{\text{HQ}}^2}{s} e^{2\zeta}\right)^{-2} \frac{1}{k_{\perp}' \cosh \zeta}, \end{aligned} \quad (27)$$

where we have used the rapidity integration limits as $\zeta_1 = 20$.

III. RESULTS AND DISCUSSION

To perform the numerical computation of various transport coefficients of HQs, we need to fix first the Gribov mass parameter γ_G . This has been achieved via determining the equilibrium thermodynamics quantities of Gribov plasma [94] and doing the matching of the said quantities with the scaled trace anomaly results obtained through lattice [108]. Fig. 2 shows the dependence of scaled Gribov parameter γ_G/T with temperature T , which is in accord with the theoretical calculations in the high-temperature limit [89]. This dependence has been utilized in the transport coefficient through interaction elements presented in appendix A. We now discuss the numerically estimated results for the drag and diffusion coefficients, energy loss, and nuclear modification factor of the charm quark, particularly having mass 1.3 GeV in an anisotropic medium, in separate subsections.

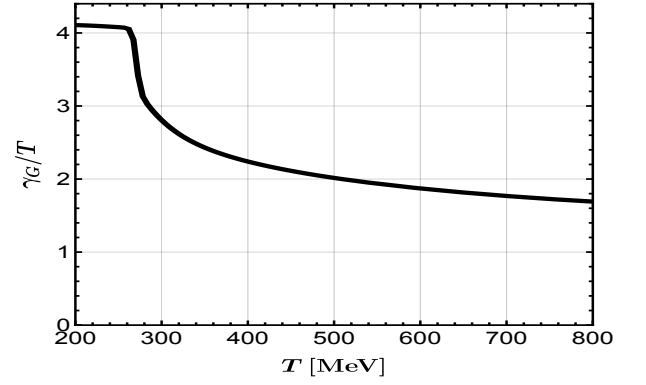


FIG. 2: Temperature dependence of scaled Gribov mass parameter γ_G/T determined via lattice (thermodynamics) data [108].

A. Transport coefficients in anisotropic medium

To consider the anisotropy effects, we have considered the weak anisotropy scenario where ξ can take 0.2, 0.3, 0.4 values only, which have been obtained through the hydrodynamic simulation approach [109, 110]. In Fig. 3a, we have plotted the drag coefficient in an anisotropic medium for a particular anisotropy parameter $\xi = 0.3$ and for various directional anisotropies accounting for both the collisional and radiative contributions combined. It can be observed that the HQs suffers a lesser hindrance in an anisotropic medium compared to an isotropic one. Also, the presence of hindrance will become much less for the lower momentum regime as the directional anisotropy increases, as can be seen in Fig. 3a. The momentum dependence of diffusion coefficient component $\mathcal{B}_0^a = \mathcal{B}_0 + \delta\mathcal{B}_0$ is shown in Fig. 3b where anisotropy lowers the \mathcal{B}_0^a component magnitude for higher momentum values significantly compared to lower momentum values. The directional anisotropy does not significantly affect momentum diffusion \mathcal{B}_0^a . In Fig. 4a, we have shown how the ratio of anisotropic correction to isotropic contribution varies with the HQ momentum. It can be seen that the said ratio depends strongly on the anisotropy strength and directional anisotropy for lower momentum values compared to the high-momentum regime. The anisotropic correction with respect to the isotropic contribution to the drag coefficient reduces as the anisotropy strength increases along with the increase in the angle between the anisotropy direction (Θ_n) and the HQ motion direction. The other drag coefficient, which solely arises due to anisotropy effects, has been plotted in Figs. 4b and 4c for RHIC and LHC energies, respectively, which shows a diminishing dependence on high-momentum values. Again, the anisotropy strength plays a key role in the additional drag component, which is more significant at LHC energies compared to RHIC energies. Note that here we have added both the collisional and the radiative contributions by considering the nonperturbative effects via the Gribov-Zwanziger propagator, contrary to

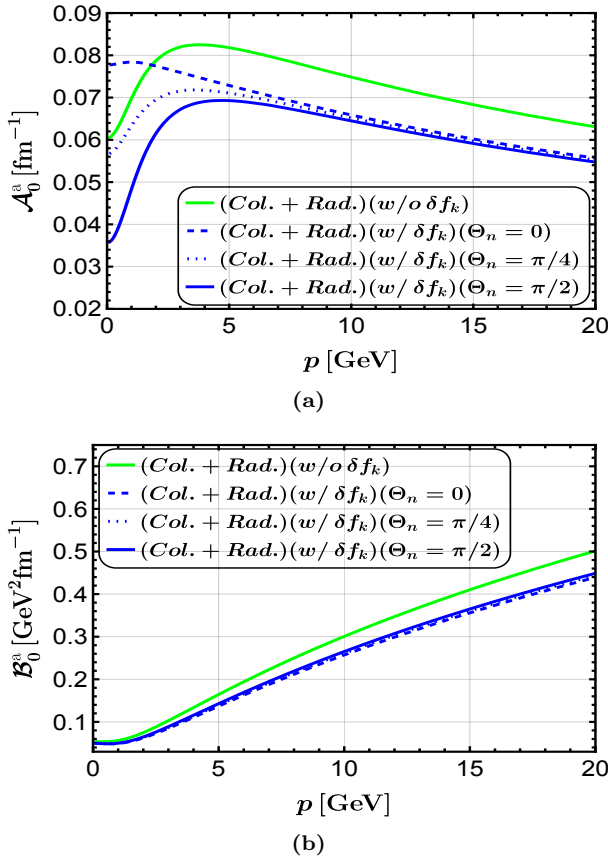


FIG. 3: *Upper panel:* Momentum variation of total drag coefficient in an anisotropic medium for different directional anisotropies. *Lower panel:* Total HQ diffusion coefficient \mathcal{B}_0^a variation with momentum. Both drag and diffusion coefficients are calculated for $T = 360$ MeV.

the earlier perturbative results where only the collisional contribution has been included in [53] and radiative processes effects have been considered in [54].

The anisotropic corrections for the components $\mathcal{B}_0^a = \mathcal{B}_0 + \delta B_0$ and $\mathcal{B}_1^a = \mathcal{B}_1 + \delta B_1$ with respect to isotropic HQ diffusion coefficient has been shown in Figs. 5a and 5b, respectively at $T = 360$ MeV. For both diffusion components, the anisotropy parameter ξ has a strong dependence and thus lowers the diffusion components significantly. Also for the component \mathcal{B}_0^a got an extra anisotropic contribution compared to \mathcal{B}_1^a as can be seen from the Eq. (17). It has been observed that the directional anisotropy is more prominent for the intermediate and the higher momentum regime for $\delta \mathcal{B}_0$ component compared to $\delta \mathcal{B}_1$ component.

In Fig. 6a, we have plotted the relative correction to the HQ diffusion coefficient namely \mathcal{B}_1^a . It has been found that the diffusion component \mathcal{B}_1^a is roughly same with \mathcal{B}_0^a for low-momentum regime. At the same time, a substantial deviation has been observed for different directional anisotropies for high-momentum regimes. The other two diffusion components, \mathcal{B}_2^a and \mathcal{B}_3^a , which arises

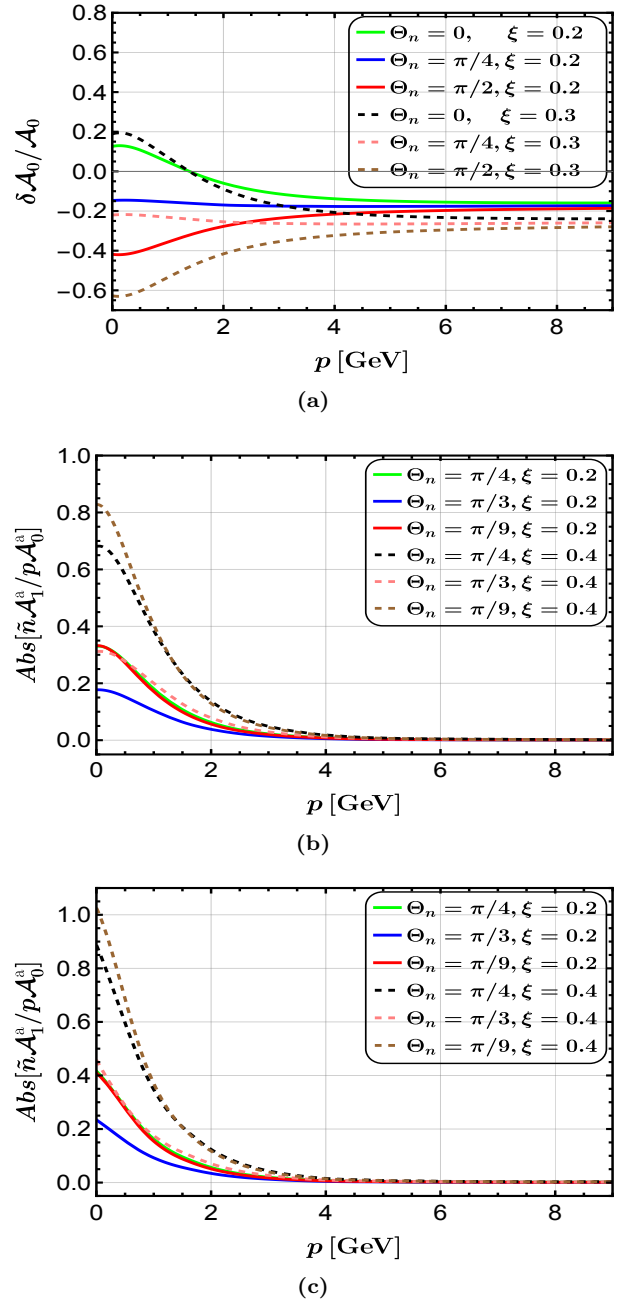


FIG. 4: *Upper panel:* Momentum dependence for the ratio of anisotropic correction to the isotropic drag coefficient for $T = 360$ MeV. *Middle panel:* The relative significance of \mathcal{A}_1^a with \mathcal{A}_0^a for $T = 360$ MeV. *Lower panel:* The relative significance of \mathcal{A}_1^a with \mathcal{A}_0^a for $T = 480$ MeV.

only due to anisotropy effects have been plotted relatively with respect to \mathcal{B}_0^a in Figs. 6b and 6c respectively which shows that the anisotropy parameter ξ and directional anisotropy parameter Θ_n affects the \mathcal{B}_2^a component more compared to \mathcal{B}_3^a .

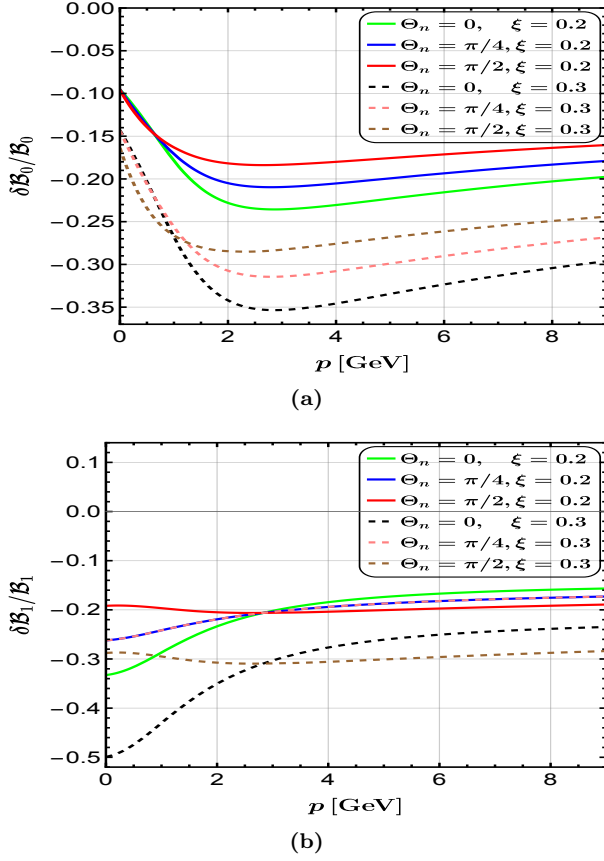


FIG. 5: *Upper panel:* Momentum variation of anisotropic correction to isotropic diffusion coefficient for B_0 . *Lower panel:* Momentum variation of anisotropic correction to isotropic diffusion coefficient for B_1 .

B. Energy loss of HQs in an anisotropic medium

As HQs traverses through the anisotropic QCD medium, the energy dissipation of HQs occurs mainly through collisional and radiative processes, and this differential energy loss can be described through the HQ drag coefficient in the following manner [111]

$$\left(\frac{dE}{dx}\right)_a = \mathcal{A}_0^a(p^2, T). \quad (28)$$

The other drag component, namely $\mathcal{A}_1^a(p^2, T)$ will not contribute to the present analysis since we are considering the energy loss in the direction of HQ initial momentum. Thus, the anisotropy contribution comes through δA_0 only as $p \cdot \tilde{n} = 0$. In Fig. 7, we have plotted the momentum dependence of the ratio of relative energy loss, i.e., anisotropic correction to energy loss $(dE/dx)_a$ with the isotropic contribution $(dE/dx)_0$ for the RHIC and LHC energies. It can be observed that the direction of anisotropy plays a key role along with the strength of the anisotropy since the said ratio of energy loss gets suppressed with an increase in the anisotropy strength. Also, directional anisotropy contributes more to lower

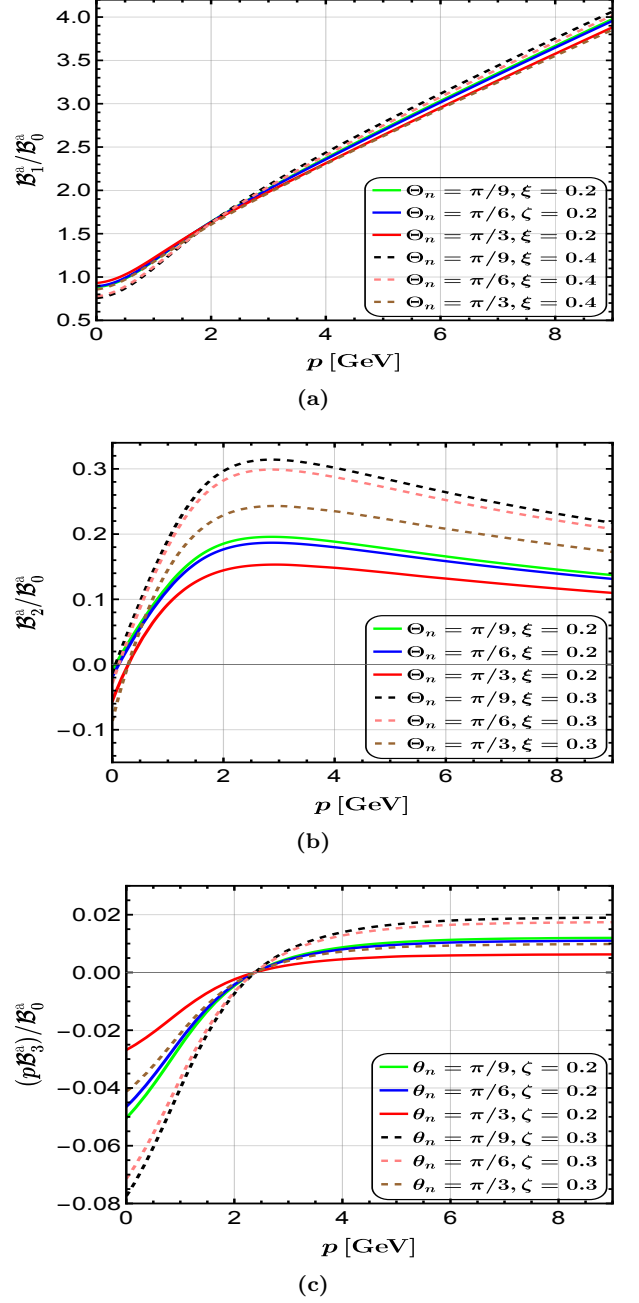


FIG. 6: Momentum variation of the ratio of different diffusion coefficient components, namely B_1 (*upper panel*), B_2 (*middle panel*) and B_3 (*lower panel*) with B_0 at $T = 360$ MeV.

momentum regimes than to higher momentum values, and again, directional anisotropy suppresses the energy loss ratio. The same observations hold for the LHC energies as well, with more clarity.

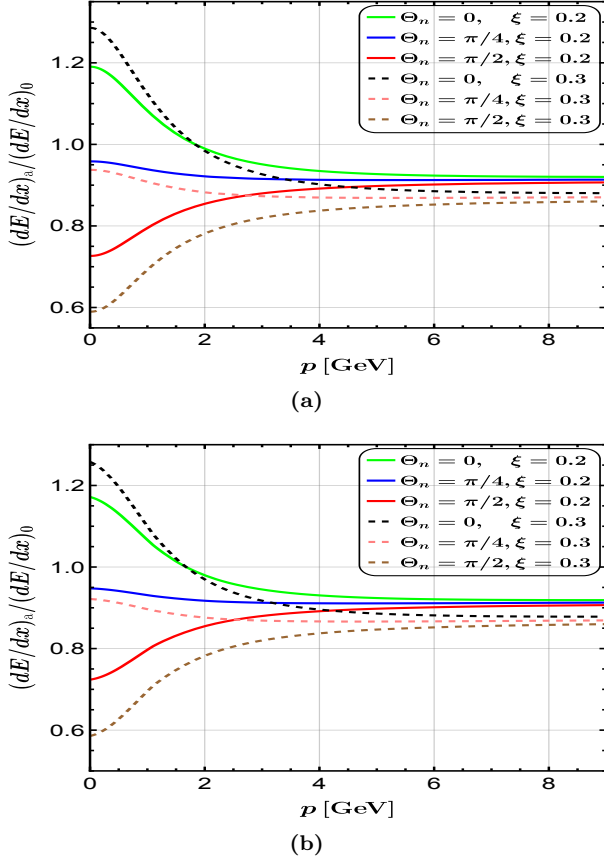


FIG. 7: Relative significance of the HQ energy loss for different weak anisotropy strengths at RHIC (*upper panel*) and LHC energy (*lower panel*).

C. Nuclear Modification factor, R_{AA}

We have investigated how momentum anisotropy influences the R_{AA} of HQs in anisotropic media. We have defined the $R_{AA}(p_T)$ as follows,

$$R_{AA}(p_T) = \frac{f_{\tau_f}(p_T)}{f_{\tau_0}(p_T)}, \quad (29)$$

where $f_{\tau_f}(p_T)$ represents the momentum distribution of charm quarks after evolving for a time $\tau_f = 5$ fm/c, and $f_{\tau_0}(p_T)$ corresponds to the initial momentum distribution of charm quarks. The initial distribution is taken from Fixed Order + Next-to-Leading Log (FONLL) calculations, which accurately describe the production spectra of D-mesons in proton-proton collisions via fragmentation processes [112, 113]. The initial momentum spectrum is parameterized as

$$\frac{dN}{d^2p_T} = \frac{x_0}{(x_1 + p_T)^{x_2}}, \quad (30)$$

with the parameters $x_0 = 6.365480 \times 10^8$, $x_1 = 9.0$, and $x_2 = 10.27890$. A deviation of $R_{AA}(p_T)$ from unity indicates that charm quarks interact with the medium, re-

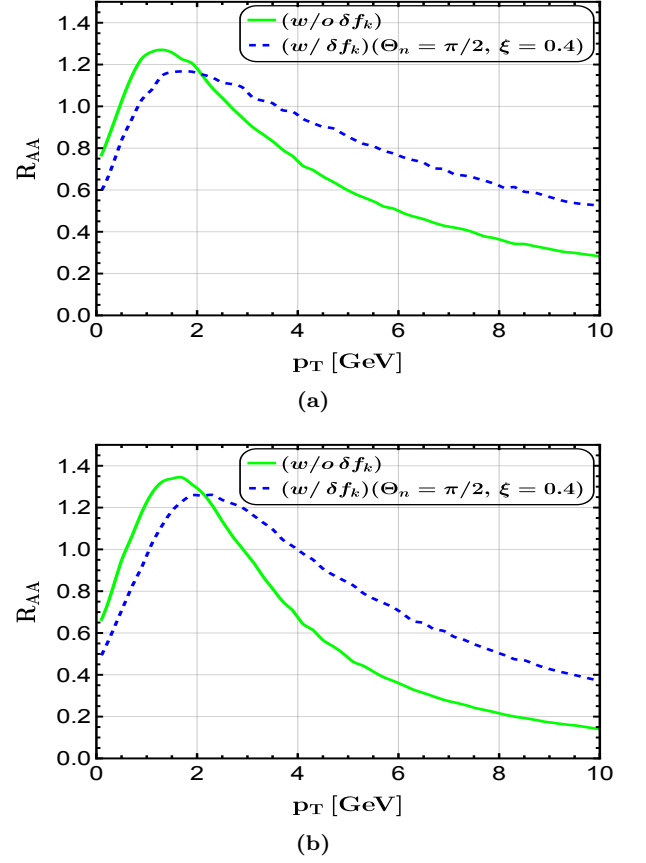


FIG. 8: Nuclear modification factor (R_{AA}) is plotted as a function of transverse momentum (p_T) for a QGP evolution time $\tau_f = 5$ fm/c. Results are shown at two temperatures: $T = 360$ MeV (*upper panel*) and $T = 480$ MeV (*lower panel*) considering collisional and radiation combined processes.

sulting in significant alterations to their momentum spectra. These interactions reflect the medium's influence on the dynamics of charm quarks. The standard method for studying the momentum evolution of the HQ in a medium involves evaluating the Fokker-Planck equation using a stochastic approach based on Langevin dynamics. The corresponding Langevin equation of motion for the HQ is given by [17]

$$dx_i = \frac{p_i}{E} dt, \quad (31a)$$

$$dp_i = -\mathcal{A} p_i dt + C_{ij} \rho_j \sqrt{dt}, \quad (31b)$$

Here, dx_i and dp_i represent the respective changes in position and momentum over each time interval dt . The drag coefficient is denoted by \mathcal{A} . C_{ij} represents the covariance matrix, and ρ_j is a Gaussian-distributed random variable with $\langle \rho_i \rho_j \rangle = \delta_{ij}$ and $\langle \rho_i \rangle = 0$. The matrix C_{ij} is expressed as

$$C_{ij} = \sqrt{2\mathcal{B}_0} \left(\delta_{ij} - \frac{p_i p_j}{p^2} \right) + \sqrt{2\mathcal{B}_1} \frac{p_i p_j}{p^2} \mathcal{B}_1. \quad (32)$$

In the limit $\mathcal{B}_0 = \mathcal{B}_1 = \mathcal{B}$, we have $C_{ij} = \sqrt{2\mathcal{B}} \delta_{ij}$. While this isotropic approximation is rigorously valid only in

the static limit ($p \rightarrow 0$), it remains widely utilized for modeling HQ motion at finite momentum in the QGP medium [11, 17, 19].

We have calculated R_{AA} to assess the effects of the Gribov gluon plasma in the presence of an anisotropic medium. The results are shown in Fig. 8 for two temperature values: 360 MeV (*Upper panel*), corresponding to RHIC energies, and 480 MeV, corresponding to LHC energies (*Lower panel*). A static medium is assumed with a lifetime of $\tau_f=5$ fm/c as the characteristic lifetime of the QGP typically expected in high-energy nuclear collisions at RHIC and LHC energies. The impact of momentum anisotropy is evaluated for an anisotropy angle $\Theta_n = \pi/2$ and an anisotropy strength $\xi = 0.4$. The effects of collisional and radiative energy loss mechanisms are incorporated for both isotropic and anisotropic media. The results indicate that the suppression of R_{AA} is more pronounced in the isotropic medium than in the anisotropic medium at higher p_T .

IV. CONCLUSION

To summarize, in this work, we have investigated the behavior of HQs as they undergo both elastic and radiative energy loss while they interact with the medium constituents in an anisotropic QGP medium. We have studied the HQs dynamics for different anisotropy strengths and different directional anisotropies present in the hot QCD environment. The study examines both elastic and inelastic interactions between HQs and the medium by evaluating the corresponding drag and diffusion coefficients, employing the Fokker-Planck formalism as the theoretical framework. The medium interactions between the HQs and the medium constituents have been modeled using the Gribov propagator to incorporate nonperturbative effects. The effects of momentum anisotropy have been included through deviations in the parton equilibrium distribution function, considered in the weak-anisotropy limit. In an anisotropic medium,

the drag and diffusion processes split into multiple components due to the directional dependence introduced by the anisotropy. Specifically, the drag coefficients decompose into two distinct components, and the diffusion coefficients are decomposed into four coefficients. The matching between the thermodynamics of the Gribov plasma has been done with the pure gauge lattice results to estimate the temperature dependence of the Gribov mass parameter. This dependence has been utilized to estimate the anisotropic corrections of the drag and diffusion coefficients.

It has been deduced that in the presence of weak momentum anisotropy, the QCD medium exerts less hindrance to HQs and, further, the hindrance becomes less as the directional anisotropy increases in the medium. Also, momentum and directional anisotropy are more dominant in the lower momentum regime than in higher momentum values for both drag coefficient components. For various diffusion coefficients, the degree of momentum anisotropy and the angular dependence between the anisotropy vector and the HQ momentum direction significantly influence their estimation. The drag and diffusion coefficients obtained via the Fokker-Planck equation are utilized to calculate the energy loss and R_{AA} of the HQs, and it has been found that the anisotropy strength and directional anisotropy suppress the energy loss for both RHIC and LHC energies. Also, R_{AA} is more pronounced at higher transverse momentum p_T in the isotropic medium compared to the anisotropic medium. It will be interesting to study the elliptic flow coefficient (v_2) of HQs in an anisotropic background, where the effects of anisotropy may play a significant role. We will address this aspect in a subsequent publication.

As a further extension, we aim to investigate the role of bulk viscosity in the HQ transport coefficients and their implications for experimental signatures such as R_{AA} , and v_2 . Such an analysis could deepen our understanding of QGP transport behavior in extreme environments. To this end, we plan to incorporate bulk viscous effects through nonequilibrium modifications to the distribution functions of medium partons within the current theoretical framework [49].

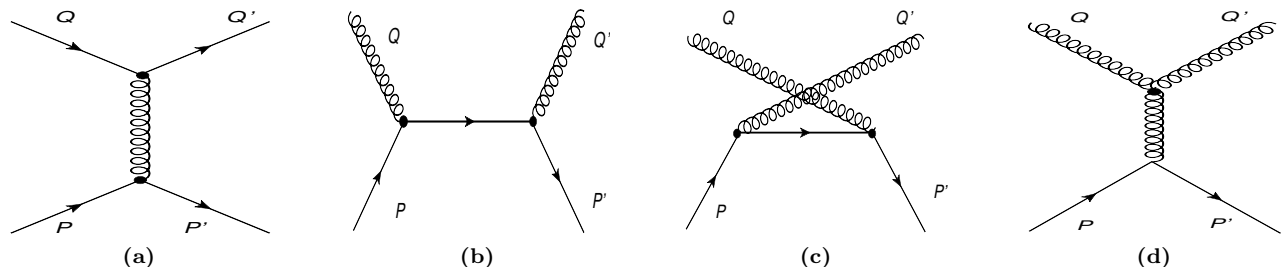


FIG. 9: Feynman graphs for the HQ elastic scattering interaction with (a) gluon (t -type exchange), (b) gluon (s -type exchange), (c) gluon (u -type exchange), (d) light quark/anti-quark (t -type exchange).

Appendix A: SCATTERING ELEMENTS FOR ELASTIC PROCESSES

(i) For the scattering $HQ(P) + g(Q) \rightarrow HQ(P') + g(Q')$, as depicted in the Fig. 9, the matrix elements reads as

$$|\mathcal{M}_{(a)}|^2 = \gamma_{HQ} \gamma_g \left[\frac{32\pi^2 \alpha^2 (s - M_{HQ}^2) (M_{HQ}^2 - u) t^2}{(t^2 + \gamma_G^4)^2} \right], \quad (A1a)$$

$$|\mathcal{M}_{(b)}|^2 = \gamma_{HQ} \gamma_g \left[\frac{64\pi^2 \alpha^2 (s - M_{HQ}^2) (M_{HQ}^2 - u) + 2M_{HQ}^2 (s + M_{HQ}^2)}{9 (s - M_{HQ}^2)^2} \right], \quad (A1b)$$

$$|\mathcal{M}_{(c)}|^2 = \gamma_{HQ} \gamma_g \left[\frac{64\pi^2 \alpha^2 (s - M_{HQ}^2) (M_{HQ}^2 - u) + 2M_{HQ}^2 (M_{HQ}^2 + u)}{9 (M_{HQ}^2 - u)^2} \right], \quad (A1c)$$

$$\mathcal{M}_{(a)} \mathcal{M}_{(b)}^* = \mathcal{M}_{(b)}^* \mathcal{M}_{(a)} = \gamma_{HQ} \gamma_g \left[\frac{8\pi^2 \alpha^2 (s - M_{HQ}^2) (M_{HQ}^2 - u) + M_{HQ}^2 (s - u)}{\left(\frac{t^2 + \gamma_G^4}{t}\right) (s - M_{HQ}^2)} \right], \quad (A1d)$$

$$\mathcal{M}_{(a)} \mathcal{M}_{(c)}^* = \mathcal{M}_{(c)}^* \mathcal{M}_{(a)} = \gamma_{HQ} \gamma_g \left[\frac{8\pi^2 \alpha^2 (s - M_{HQ}^2) (M_{HQ}^2 - u) - M_{HQ}^2 (s - u)}{\left(\frac{t^2 + \gamma_G^4}{t}\right) (M_{HQ}^2 - u)} \right], \quad (A1e)$$

$$\mathcal{M}_{(b)} \mathcal{M}_{(c)}^* = \mathcal{M}_{(c)}^* \mathcal{M}_{(b)} = \gamma_{HQ} \gamma_g \left[\frac{8\pi^2 \alpha^2}{9} \frac{M_{HQ}^2 (4M_{HQ}^2 - t)}{(s - M_{HQ}^2) (M_{HQ}^2 - u)} \right], \quad (A1f)$$

$$|\mathcal{M}_{(i)}|^2 = |\mathcal{M}_{(a)}|^2 + |\mathcal{M}_{(b)}|^2 + |\mathcal{M}_{(c)}|^2 + 2\mathcal{R}e\{\mathcal{M}_{(a)} \mathcal{M}_{(b)}^*\} + 2\mathcal{R}e\{\mathcal{M}_{(b)} \mathcal{M}_{(c)}^*\} + 2\mathcal{R}e\{\mathcal{M}_{(a)} \mathcal{M}_{(c)}^*\}, \quad (A1g)$$

and (ii) for the scattering $HQ(P) + lq(Q)/l\bar{q}(Q) \rightarrow HQ(P') + lq(Q')/l\bar{q}(Q')$, one obtains

$$|\mathcal{M}_{(d)}|^2 = \gamma_{HQ} \gamma_{lq/l\bar{q}} \left[\frac{64\pi^2 \alpha^2 \left\{ (s - M_{HQ}^2)^2 + (M_{HQ}^2 - u)^2 + 2M_{HQ}^2 \frac{t^2 + \gamma_G^4}{t} \right\} t^2}{9 (t^2 + \gamma_G^4)^2} \right]. \quad (A2)$$

Here, $\gamma_{HQ} = N_s \times N_c$, $\gamma_g = N_s \times (N_c^2 - 1)$ and $\gamma_{lq/l\bar{q}} = N_s \times N_c \times N_f$ are the statistical degeneracy for the HQ, gluon, and light quark particles respectively with $N_s = 2$, $N_f = 3$ and $N_c = 3$ have been considered.

Appendix B: PROJECTIONS OF ANISOTROPY VECTORS IN THE COM

The various projection mentioned in Eq. (20) are defined as follow as

$$(\mathbf{x}_{cm} \cdot \mathbf{n}) = \frac{\gamma_{cm}}{p_{cm}} \left[p \cos \Theta_n - E_p \frac{(p \cos \Theta_n + q \cos \chi \cos \Theta_n + q \sin \chi \cos \Phi \sin \Theta_n)}{E_p + E_q} \right], \quad (B1a)$$

$$(\mathbf{y}_{cm} \cdot \mathbf{n}) = N^{-1} \left[\frac{p \cos \Theta_n + q \cos \chi \cos \Theta_n + q \sin \chi \cos \Phi \sin \Theta_n}{E_p + E_q} \right] - (\mathbf{v}_{cm} \cdot \mathbf{p}_{cm}) \frac{\gamma_{cm}}{p_{cm}} \left[p \cos \Theta_n - E_p \frac{(p \cos \Theta_n + q \cos \chi \cos \Theta_n + q \sin \chi \cos \Phi \sin \Theta_n)}{E_p + E_q} \right], \quad (B1b)$$

$$(\mathbf{z}_{cm} \cdot \mathbf{n}) = \gamma_{cm} N^{-1} \frac{1}{p_{cm} (E_p + E_q)} p q \sin \chi \sin \Phi \sin \Theta_n, \quad (B1c)$$

$$(\mathbf{x}_{cm} \cdot \mathbf{p}) = \frac{\gamma_{cm}}{p_{cm}} \left[p^2 - E_p \frac{(p^2 + p q \cos \chi)}{(E_p + E_q)} \right], \quad (B1d)$$

$$(\mathbf{y}_{cm} \cdot \mathbf{p}) = N^{-1} \left[\frac{p^2 + p q \cos \chi}{(E_p + E_q)} - (\mathbf{v}_{cm} \cdot \mathbf{p}_{cm}) \frac{\gamma_{cm}}{p_{cm}^2} \left(p^2 - \frac{E_p (p^2 + p q \cos \chi)}{E_p + E_q} \right) \right]. \quad (B1e)$$

-
- [1] E. V. Shuryak, Nucl. Phys. A **750** (2005), 64-83
 - [2] P. Bozek and I. Wyskiel-Piekarska, Phys. Rev. C **83**, 024910 (2011)
 - [3] W. Jas and S. Mrowczynski, Phys. Rev. C **76**, 044905 (2007)
 - [4] W. Florkowski, R. Ryblewski and M. Strickland, Phys. Rev. C **88**, 024903 (2013)
 - [5] A. Kurkela and G. D. Moore, JHEP **12**, 044 (2011)
 - [6] A. Kurkela and G. D. Moore, JHEP **11**, 120 (2011)
 - [7] M. Attems, A. Rebhan and M. Strickland, Phys. Rev. D **87**, no.2, 025010 (2013)
 - [8] A. Ipp, A. Rebhan and M. Strickland, Phys. Rev. D **84**, 056003 (2011)
 - [9] S. Guin, H. Pandey and S. Sharma, Phys. Lett. B **866**, 139490 (2025)
 - [10] S. Mrowczynski, B. Schenke and M. Strickland, Phys. Rept. **682**, 1-97 (2017)
 - [11] R. Rapp, P. B. Gossiaux, A. Andronic, R. Averbeck, S. Masiocchi, *et al.* Nucl. Phys. A **979**, 21-86 (2018)
 - [12] S. K. Das, J. M. Torres-Rincon and R. Rapp, Phys. Rept. **1129**, 1131 (2025)
 - [13] A. M. Sirunyan *et al.* [CMS], Phys. Lett. B **782**, 474-496 (2018)
 - [14] S. Acharya *et al.* [ALICE], JHEP **01**, 174 (2022)
 - [15] J. Adam *et al.* [STAR], Phys. Rev. C **99**, no.3, 034908 (2019)
 - [16] B. Svetitsky, Phys. Rev. D **37**, 2484-2491 (1988)
 - [17] G. D. Moore and D. Teaney, Phys. Rev. C **71**, 064904 (2005)
 - [18] H. van Hees and R. Rapp, Phys. Rev. C **71**, 034907 (2005)
 - [19] H. van Hees, V. Greco and R. Rapp, Phys. Rev. C **73**, 034913 (2006)
 - [20] J. Zhao, K. Zhou, S. Chen and P. Zhuang, Prog. Part. Nucl. Phys. **114**, 103801 (2020)
 - [21] M. He, R. J. Fries and R. Rapp, Phys. Lett. B **735**, 445-450 (2014)
 - [22] S. K. Das, F. Scardina, S. Plumari and V. Greco, Phys. Lett. B **747**, 260-264 (2015)
 - [23] T. Song, H. Berrehrh, D. Cabrera, J. M. Torres-Rincon, *et al.* Phys. Rev. C **92**, no.1, 014910 (2015)
 - [24] S. Cao, G. Coci, S. K. Das, W. Ke, S. Y. F. Liu, S. Plumari, *et al.* Phys. Rev. C **99**, no.5, 054907 (2019)
 - [25] E. Iancu, A. Leonidov and L. D. McLerran, Nucl. Phys. A **692**, 583-645 (2001)
 - [26] C. Tsallis, J. Statist. Phys. **52**, 479-487 (1988)
 - [27] T. Song, K. C. Han and C. M. Ko, Phys. Rev. C **85**, 054905 (2012)
 - [28] J. Aichelin and K. Werner, J. Phys. G **37**, 094006 (2010)
 - [29] Y. L. Dokshitzer and D. E. Kharzeev, Phys. Lett. B **519** (2001), 199-206
 - [30] R. Abir, U. Jamil, M. G. Mustafa and D. K. Srivastava, Phys. Lett. B **715** (2012), 183-189
 - [31] E. Braaten and M. H. Thoma, Phys. Rev. D **44** (1991), 1298-1310
 - [32] E. Braaten and M. H. Thoma, Phys. Rev. D **44** (1991) no.9, R2625
 - [33] M. G. Mustafa, D. Pal, D. K. Srivastava and M. Thoma, Phys. Lett. B **428** (1998), 234-240
 - [34] M. G. Mustafa, Phys. Rev. C **72** (2005), 014905
 - [35] G. Y. Qin, J. Ruppert, C. Gale, S. Jeon, G. D. Moore and M. G. Mustafa, Phys. Rev. Lett. **100** (2008), 072301
 - [36] S. Mazumder, T. Bhattacharyya, J. e. Alam and S. K. Das, Phys. Rev. C **84** (2011), 044901
 - [37] M. Ruggieri, Pooja, J. Prakash and S. K. Das, Phys. Rev. D **106** (2022) no.3, 034032
 - [38] S. K. Das, P. Palni, A. Sarkar, V. K. Agotiya, A. Bandyopadhyay, *et al.* [arXiv:2412.14026 [nucl-ex]].
 - [39] S. K. Das, P. Palni, J. Sannigrahi, J. e. Alam, *et al.* Int. J. Mod. Phys. E **31** (2022), 12
 - [40] J. Prakash and M. Y. Jamal, Eur. Phys. J. Plus **139** (2024) no.9, 778
 - [41] X. N. Wang, M. Gyulassy and M. Plumer, Phys. Rev. D **51** (1995), 3436-3446
 - [42] M. Gyulassy and X. n. Wang, Nucl. Phys. B **420** (1994), 583-614
 - [43] S. Klein, Rev. Mod. Phys. **71** (1999), 1501-1538
 - [44] R. Abir, *et al.* Phys. Rev. D **85** (2012), 054012
 - [45] Y. Guo, L. Qiu, R. Zhao and M. Strickland, Phys. Rev. D **109**, no.11, 114025 (2024)
 - [46] L. Dong, Y. Guo, A. Islam, A. Rothkopf and M. Strickland, JHEP **09**, 200 (2022)
 - [47] L. Thakur and Y. Hirono, JHEP **02** (2022), 207
 - [48] S. K. Das, V. Chandra and J. e. Alam, J. Phys. G **41** (2013), 015102
 - [49] L. Thakur, N. Haque and Y. Hirono, JHEP **06** (2020), 071
 - [50] A. Shaikh, M. Kurian, S. K. Das, V. Chandra, S. Dash and B. K. Nandi, Phys. Rev. D **104** (2021) no.3, 034017
 - [51] B. Singh and H. Mishra, Phys. Rev. D **101** (2020) no.5, 054027
 - [52] M. E. Carrington, A. Czajka and S. Mrowczynski, Phys. Rev. C **105**, no.6, 064910 (2022)
 - [53] A. Kumar, M. Kurian, S. K. Das and V. Chandra, Phys. Rev. C **105** (2022) no.5, 054903
 - [54] J. Prakash, V. Chandra and S. K. Das, Phys. Rev. D **108** (2023) no.9, 096016
 - [55] Q. Du, M. Du and Y. Guo, Phys. Rev. D **110**, no.3, 034011 (2024)
 - [56] M. E. Carrington, K. Deja and S. Mrowczynski, Phys. Rev. C **92**, no.4, 044914 (2015)
 - [57] S. K. Das, M. Ruggieri, F. Scardina, S. Plumari and V. Greco, J. Phys. G **44**, no.9, 095102 (2017)
 - [58] T. Song, P. Moreau, J. Aichelin and E. Bratkovskaya, Phys. Rev. C **101**, no.4, 044901 (2020)
 - [59] H. Pandey, S. Schlichting and S. Sharma, Phys. Rev. Lett. **132**, no.22, 222301 (2024)
 - [60] K. Boguslavski, A. Kurkela, T. Lappi, F. Lindenbauer and J. Peuron, Phys. Rev. D **109**, no.1, 014025 (2024)
 - [61] K. Boguslavski, A. Kurkela, T. Lappi and J. Peuron, JHEP **09**, 077 (2020)
 - [62] H. Pandey, S. Schlichting and S. Sharma, J. Subatomic Part. Cosmol. **3**, 100034 (2025)
 - [63] P. Romatschke and M. Strickland, Phys. Rev. D **68**, 036004 (2003)
 - [64] M. E. Carrington, K. Deja and S. Mrowczynski, Phys. Rev. C **90**, no.3, 034913 (2014)
 - [65] P. K. Srivastava, L. Thakur and B. K. Patra, Phys. Rev. C **91**, no.4, 044903 (2015)
 - [66] M. Y. Jamal, S. Mitra and V. Chandra, Phys. Rev. D **95**, no.9, 094022 (2017)
 - [67] A. Kumar, M. Y. Jamal, V. Chandra and J. R. Bhatt,

- Phys. Rev. D **97**, no.3, 034007 (2018)
- [68] R. Ghosh, B. Karmakar and A. Mukherjee, Phys. Rev. D **102**, no.11, 114002 (2020)
 - [69] R. Zhao, L. Qiu, Y. Guo and M. Strickland, Phys. Rev. D **108**, no.3, 3 (2023)
 - [70] S. Mrowczynski, Eur. Phys. J. A **54**, no.3, 43 (2018)
 - [71] M. Ruggieri and S. K. Das, Phys. Rev. D **98**, no.9, 094024 (2018)
 - [72] P. Khowal, S. K. Das, L. Oliva and M. Ruggieri, Eur. Phys. J. Plus **137**, no.3, 307 (2022)
 - [73] H. van Hees, M. Mannarelli, V. Greco and R. Rapp, Phys. Rev. Lett. **100**, 192301 (2008)
 - [74] V. Greco, C. M. Ko and R. Rapp, Phys. Lett. B **595** (2004), 202-208
 - [75] V. Greco, C. M. Ko and P. Levai, Phys. Rev. Lett. **90** (2003), 202302
 - [76] P. B. Gossiaux and J. Aichelin, Phys. Rev. C **78** (2008), 014904
 - [77] S. Plumari, W. M. Alberico, V. Greco and C. Ratti, Phys. Rev. D **84** (2011), 094004
 - [78] H. Berrehrah, P. B. Gossiaux, J. Aichelin, W. Cassing, *et al.* Phys. Rev. C **90** (2014) no.6, 064906
 - [79] F. Scardina, S. K. Das, V. Minissale, S. Plumari and V. Greco, Phys. Rev. C **96**, no.4, 044905 (2017)
 - [80] V. N. Gribov, Nucl. Phys. B **139** (1978), 1
 - [81] D. Zwanziger, Nucl. Phys. B **323** (1989), 513-544
 - [82] A. D. Linde, Phys. Lett. B **96**, 289-292 (1980)
 - [83] N. Vandersickel and D. Zwanziger, Phys. Rept. **520**, 175-251 (2012)
 - [84] M. Tissier and N. Wschebor, Phys. Rev. D **82**, 101701 (2010)
 - [85] B. W. Mintz, L. F. Palhares, G. Peruzzo and S. P. Sorella, Phys. Rev. D **99**, no.3, 034002 (2019)
 - [86] M. Peláez, U. Reinosa, J. Serreau, *et al.* Rept. Prog. Phys. **84**, no.12, 124202 (2021)
 - [87] D. Zwanziger, Phys. Rev. Lett. **94**, 182301 (2005)
 - [88] D. Zwanziger, Phys. Rev. D **76**, 125014 (2007)
 - [89] K. Fukushima and N. Su, Phys. Rev. D **88** (2013), 076008
 - [90] N. Su and K. Tywoniuk, Phys. Rev. Lett. **114** (2015) no.16, 161601
 - [91] D. E. Kharzeev and E. M. Levin, Phys. Rev. Lett. **114** (2015) no.24, 242001
 - [92] W. Florkowski, R. Ryblewski, N. Su and K. Tywoniuk, Phys. Rev. C **94** (2016) no.4, 044904
 - [93] W. Florkowski, R. Ryblewski, N. Su and K. Tywoniuk, Acta Phys. Polon. B **47** (2016), 1833
 - [94] A. Jaiswal and N. Haque, Phys. Lett. B **811** (2020), 135936
 - [95] A. Bandyopadhyay, N. Haque, M. G. Mustafa and M. Strickland, Phys. Rev. D **93** (2016) no.6, 065004
 - [96] Sumit, N. Haque and B. K. Patra, Phys. Lett. B **845** (2023), 138143
 - [97] A. Bandyopadhyay, J. Phys. G **51**, no.12, 125002 (2024)
 - [98] S. Madni, A. Mukherjee, A. Jaiswal and N. Haque, Phys. Rev. D **110**, no.11, 116035 (2024)
 - [99] S. Madni, L. Thakur and N. Haque, [arXiv:2404.09767 [hep-ph]].
 - [100] Y. L. Du, N. Su and K. Tywoniuk, [arXiv:2412.20165 [hep-th]].
 - [101] M. Debnath, R. Ghosh and N. Haque, Eur. Phys. J. C **84**, no.3, 313 (2024)
 - [102] W. Wu, G. Huang, J. Zhao and P. Zhuang, Phys. Rev. D **107** (2023) no.11, 114033
 - [103] S. Madni, A. Mukherjee, A. Bandyopadhyay and N. Haque, Phys. Lett. B **838** (2023), 137714
 - [104] Sumit, A. Mukherjee, N. Haque and B. K. Patra, Phys. Rev. D **109**, no.11, 11 (2024)
 - [105] S. Mazumder, N. Sharma and L. Kumar, Phys. Rev. C **111**, no.3, 034905 (2025)
 - [106] M. Debnath, R. Ghosh, M. Y. Jamal, M. Kurian and J. Prakash, Phys. Rev. D **109**, no.1, L011503 (2024)
 - [107] N. Haque, A. Bandyopadhyay, J. O. Andersen, M. G. Mustafa, *et al.* JHEP **05**, 027 (2014)
 - [108] S. Borsanyi, G. Endrodi, Z. Fodor, S. D. Katz and K. K. Szabo, JHEP **07**, 056 (2012)
 - [109] T. Epelbaum and F. Gelis, Phys. Rev. Lett. **111**, 232301 (2013)
 - [110] M. Strickland, Nucl. Phys. A **926**, 92-101 (2014)
 - [111] M. Golam Mustafa, D. Pal and D. Kumar Srivastava, Phys. Rev. C **57**, 889-898 (1998)
 - [112] M. Cacciari, S. Frixione, N. Houdeau, M. L. Mangano, P. Nason and G. Ridolfi, JHEP **10**, 137 (2012)
 - [113] M. Cacciari, P. Nason and R. Vogt, Phys. Rev. Lett. **95**, 122001 (2005)